RESEARCH ARTICLE

DOI: 10.54926/jnamt.2025.2410

J Nav Architect Mar Technol 2025;227(1):34-42

Exergy Based Ecological Performance Analysis of a Waste Heat-Powered Marine Refrigeration Cycle

Oğulcan Yılmaztürk, Asım Sinan Karakurt

Yıldız Technical University Faculty of Naval Architecture and Maritime, Deparment of Naval Architecture and Marine Engineering, İstanbul, Türkiye

To cite this article: O. Yılmaztürk, and A. S. Karakurt. Exergy based ecological performance analysis of a waste heat-powered marine refrigeration cycle. *J Nav Architect Mar Technol*. 2025;227(1):34-42.

Received: 22.11.2024 - **Revised:** 20.02.2025 - **Accepted:** 18.03.2025 - **Publication Date:** 29.05.2025

Abstract

The escalating costs of fuel, global fuel supply disruptions, and stringent international emissions regulations necessitate more efficient ship operations. A key component of environmentally sustainable, economical, and efficient marine transportation is the recovery and utilization of waste heat. This study investigates the potential of converting waste heat from ship exhaust gas into useful energy through an organic Rankine cycle and its subsequent integration into a refrigeration system. In this study, the thermodynamic performance of the refrigerants R717, R152a, R290, and R134a was investigated. The findings demonstrate that R717 exhibits superior performance in terms of utilization factor and second law efficiency (η_{II}), while R290 emerges as the optimal choice when minimizing total entropy generation (s_{gen_TOT}) is the primary objective. If the priorities are focused on maximizing useful work production, minimizing energy losses, and reducing environmental impacts, the advantages of the R717 refrigerant, which has the highest total ecological coefficient of performance (ECOP) and exergetic performance criteria (EPC) values, are clearly evident. The ideal operating temperatures for evaporator temperature (T_{Evap}) and turbine temperatures ($T_{Turbine}$) concerning *EPC* and *ECOP*, using R717 as the refrigerant, were investigated in the continuation of the study. During this investigation, changes in T_{Evap} and $T_{Turbine}$ were observed to have affected other components. When the T_{Evap} is kept constant, and the $T_{Turbine}$ amount is increased, an improvement was observed in EPC_{TOT}, $ECOP_{TOT}$, η_{II}, and utility factor values, while an increase in s_{gen_TOT} and exergy destruction (ExD_{TOT}) values. When the $T_{Turbine}$ is kept constant, a decrease is observed in the EPC_{TOT} value. At the same time, an improvement is seen in ExD_{TOT}, η_{II}, and $ECOP_{TOT}$ values, while an increase is noted in the s_{gen_TOT} value.

Keywords: ECOP, EPC, heat-powered refrigeration, temperature management, waste heat recovery

1. Introduction

Contemporary engineering systems must prioritize cost-effectiveness, efficiency, and environmental sustainability. To reach these objectives, various strategies for enhancing efficiency and minimizing environmental impact are implemented throughout land and marine vehicles' design and operational phases. In the maritime domain, common approaches include resistance reduction techniques, the adoption of alternative fuels, operational optimizations, design parameters such as energy efficiency design index and energy efficiency existing index, and the recovery and utilization of waste heat [1]. Ships often generate substantial waste heat from systems like main engine cooling, lubrication, and flue gas [2]. This heat can be harnessed for various applications, including direct heating of tanks or fuel, steam generation [3], power generation, or cooling

Address for Correspondence: Asım Sinan Karakurt, Yıldız Technical University Faculty of Naval Architecture and Maritime, Deparment of Naval Architecture and Marine Engineering, İstanbul, Türkiye

E-mail: asinan@yildiz.edu.tr

ORCID ID: orcid.org/0000-0002-6205-9089

Copyright© 2025 The Author. Published by Galenos Publishing House on behalf of UCTEA Turkish Chamber of Naval Architects and Marine Engineers.
Licensed under a Creative Commons Attribution-NonCommercial-NoDerivatives 4.0 (CC BY-NC-ND) International License

through different thermodynamic cycles [4]. However, ships also face significant cooling demands for spaces, food stores, and transported cargo [5]. To meet these cooling needs, engineers explore alternative approaches beyond traditional vapor compression refrigeration (VCR) systems. These include absorption or organic Rankine cycle (ORC) driven VCR systems utilizing waste heat, as well as hybrid methods combining both approaches.

The existing literature encompasses a diverse range of investigations into ORC-driven combined cooling systems or dual-cycle configurations for marine applications and low-temperature heat sources. Comparative performance assessments of various heat-powered refrigeration cycles, including absorption cycles, multi-stage arrangements, and combined heat-power systems, have been reported [6]. Thermodynamic analyses of ORC-VCR systems utilizing low-temperature source heat have been conducted for different working fluids and design parameters, leading to insights into optimal fluid selection and equipment [7-9]. Optimization studies have focused on refining design and operational parameters of ORC-VCR systems based on varying working fluids and heat source temperatures [10,11]. Exergy-based performance analyses have explored the impact of different working fluids, heat sources, and system layouts on ORC-VCR system efficiency [12-14]. Experimental investigations have been conducted to evaluate the performance of ORC-VCR systems recovering waste heat from internal combustion engines [15].

Exergetic performance analysis and optimization of air refrigeration cycles based on ecological coefficient of performance (ECOP) were studied by [16]. Analyses of exergy-based performance outputs, including exergetic performance criteria (EPC) analyses, of the multipurpose refrigeration system for different design conditions were performed by [17]. A recent research study was explored the optimization of simple Brayton refrigeration models using an exergy-based approach to improve ecological function by [18]. Exergy based thermodynamic analysis and optimizations of low temperature cascade refrigeration systems applications were presented by [19,20]. The performance analysis of the heat-powered refrigeration system using marine waste heat energy on the second law of thermodynamics was carried out depends on the different design parameters by [21]. This study will evaluate the performance of a refrigeration system driven by an ORC utilizing waste heat from a ship's diesel engine. The analysis will focus on key performance metrics, including utility factor (U_f), second law efficiency (η_{II}), total entropy generation (s_{gen_TOT}), exergy destruction ratio (y), *ECOP*, and *EPC*. These metrics will be assessed under various operating conditions, considering different working fluids and different evaporator temperatures (T_{Evap}), condenser, and turbine temperatures ($T_{Turbine}$).

2. Thermodynamic Model

The waste heat-powered ORC-VCR system can be conceptualized as two interconnected subsystems that utilize a single working fluid, which can be applied in such as industrial waste heat recovery systems, combined cooling and power systems, data center cooling, or marine systems. The ORC is a thermodynamic cycle that converts heat energy into mechanical work, similar to a steam Rankine cycle but using an organic working fluid (e.g., R134a, R717, 290, etc) instead of water. The ORC component comprises a condenser, pump, waste heat boiler, and steam turbine. The VCR cycle is a standard refrigeration process that absorbs heat from a low-temperature or cooled source and rejects it at a higher temperature. The VCR subsystem includes an evaporator, compressor, condenser, and expansion valve. Figure 1 illustrates the flow diagram of the ORC-VCR system. The ORC effectively converts waste heat from the main engine exhaust gases into a net work, driving the pump and compressor. In cases where the main engine is not operating or cannot provide exhaust gas with sufficient

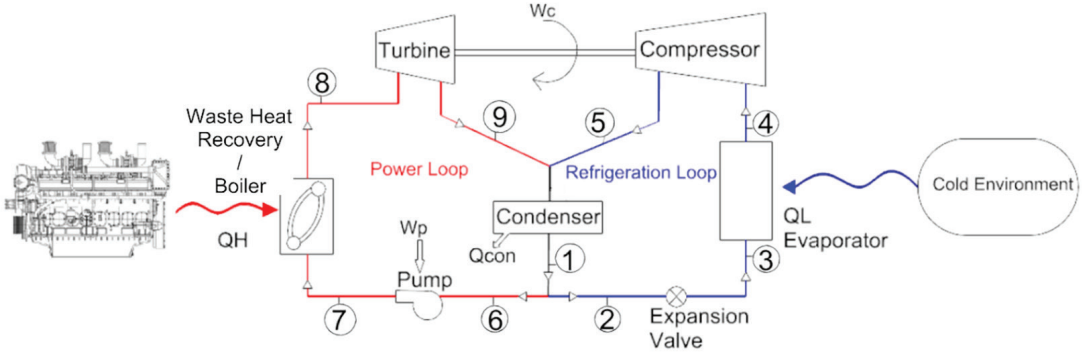


Figure 1. Thermodynamic model of the ORC-VCR system.

ORC: Organic Rankine cycle, VCR: Vapor compression refrigeration

thermal content, the boiler is activated and thus continuity in the cooling system is ensured. The VCR then leverages this energy to refrigerate the storage compartments.

The fundamental design parameters and associated assumptions are outlined below. The heat addition to the ORC, Q_H, is calculated based on exhaust gas properties, including mass flow rate and inlet temperature ($T_{exhaust,in}$). The specific heat capacity at constant temperature (Cp) of the exhaust gases was determined using Equation 1, considering the reference inlet and outlet temperatures.

$$Cp = 956 + \left(0.3389\ T_{exhaust,\,in}\right) - \left(2.476\ 10^{-5}\ T^{2}_{exhaust,\,in}\right) \quad (1)$$

Heat transfer (Q_{Con}, Q_L, and Q_H) values are calculated from the basic balance equations. The U_f, defined by Equation 2, represents the ratio of the refrigeration or cooling load of the VCR system (Q_L) to the heat input to the ORC (Q_H).

$$U_f = Q_L/Q_H \quad (2)$$

The η_{II} calculated with Equation 3 as the ratio of U_f and Carnot U_f (U_{f_Carnot}).

$$\eta_{II} = U_f/U_{f_Carnot} \quad (3)$$

s_{gen_TOT}, as defined by Equation 6, is the sum of the entropy generations from the environment, Equation 4, (Δs_{env}) and the system, Equation 5, (Δs_{sys}). The temperature difference between relevant environments and system points is denoted by ΔT. The heat transfer from the condenser unit (Q_{Con}) is the combined heat transfer from the power loop (PL) and the refrigeration loop (RL). T_{Con} and T_{avr} represent the temperature of condenser for power loop and the average value between condenser inlet and outlet temperature of RL, respectively.

$$\Delta s_{env} = \left(\left(\frac{Q_{con,\,PL}}{(T_{con} - \Delta T)}\right) + \left(\frac{Q_{con,\,RL}}{(T_{avr} - \Delta T)}\right)\right) - \left(\frac{Q_{con,\,PL}}{T_{con} + \left(\frac{Q_{con,\,RL}}{T_{avr}}\right)}\right) \quad (4)$$

$$\Delta s_{sys} = \left(\left(\frac{-Q_H}{(T_H + \Delta T)}\right) - \left(\frac{Q_L}{(T_L + \Delta T)}\right)\right) + \left(\frac{Q_H}{T_H}\right) + \left(\frac{Q_L}{T_L}\right) \quad (5)$$

$$s_{genTot} = \Delta s_{env} + \Delta s_{sys} \quad (6)$$

$$ex = h - h_0 - T_0\left(s - s_0\right) \quad (7)$$

The exergy density (ρ_{ex}) is a beneficial tool to compare the size and exergetic capacity of the system point which was defined the ratio of specific exergy to the specific volume of the system point in Equation 8 by [22].

$$\rho_{ex} = \frac{ex}{v} \quad (8)$$

The exergy destruction (ExD) of components is calculated with Equation 9 which depends on the flow rate and physical exergy of inlet and outlet conditions of components. The total ExD_{TOT} is the sum of all components of ExD as in Equation 10.

$$ExD = \dot{m}\left(ex_{in} - ex_{out}\right) \quad (9)$$

$$ExD_{TOT} = \sum ExD \quad (10)$$

The y can be defined for each component as the ratio of the ExD of components to the ExD_{TOT} of the system in Equation 11 [23].

$$y = \frac{ExD}{ExD_{TOT}} \quad (11)$$

$ECOP$ is defined as ratio of power output to the loss rate of availability in Equation 12 [24] and EPC defines the ratio of total exergy output to the loss rate of availability with Equation 13 [25].

$$ECOP = \frac{W}{T_0\, S_{gen_TOT}} \quad (12)$$

$$EPC = \frac{ex_{out}}{T_0\, s_{gen_TOT}} = \frac{ex_{out}}{ex_{in} - ex_{out}} \quad (13)$$

Some properties such as global warming potential, refrigerant concentration limit of working fluids (R717, R290, R134a, and R152a) according to the ASHRAE [26] were given in Table 1 Assumptions made for the analysis of the system were also shared in Table 2.

The thermodynamic analysis of the marine refrigeration system (MRS) was conducted for the following refrigerants: R717, R290, R134a, and R152a. The analysis relied on the following simplifying assumptions:

- All system components were assumed to operate under steady-state conditions.
- Chemical, kinetic, and potential energy, as well as their corresponding exergy terms, were disregarded.
- Pressure losses within the system's pipelines were considered negligible.
- Heat transfer to or from the compressor and expansion valve was assumed to be insignificant.
- The expansion of refrigerants in the expansion valves was assumed to be isenthalpic.

3. Results and Discussion

To evaluate the performance of the system under different refrigerant conditions, a parametric study was conducted using the established model (Equations 1-13). Four commonly employed refrigerants (R717, R290, R134a, and R152a) were selected. Their corresponding performance

Table 1. Properties of working fluids/refrigerants [26].

Fluid	*Atmospheric lifetime* (years)	*GWP* (100-yr)	ASHRAE [26] safety group	*RCL* (g/m^3)	Normal boiling point (°C)	*Critical temp.* (°C)	*Critical pressure* (kPa)
R717	0.019	0	B2L	320	-33.34	132.40	11.28
R290	13	3.3	A3	9.5	-42.10	96.70	4.25
R134a	14	1430	A1	210	-26.30	101.06	4.06
R152a	1.4	124	A2	32	-25	113.26	4.52

GWP: Global warming potential, *RCL*: Refrigerant concentration limit

Table 2. Assumptions made for the analysis of the system.

Parameters	Units	Values
Ambient temperature (T_0)	(K)	298
Ambient pressure (P_0)	(kPa)	101.325
Evaporator temperature (T_{evap})	(K)	258.15
Condenser temperature (T_{Con})	(K)	318.15
Turbine temperature ($T_{Turbine}$)	(K)	363.15
Temperature difference between cold space and evaporator (ΔT)	(K)	10

metrics, including the U_f, the η_{II}, the $ECOP_{TOT}$, the EPC_{TOT}, the s_{gen_TOT}, and the ExD_{TOT}, were calculated for different turbine and T_{Evap}. The Python 3.11.4 programming language, in conjunction with the CoolProp 8.3 library [27], was employed for the numerical simulations.

The results of this analysis, the information presented in Figure 2 compares the performance outputs of a waste heat-driven marine refrigeration cycle using four different refrigerants. It was observed that the optimal refrigerant choice is contingent upon the specific performance objective. R717 generally exhibits higher U_f, η_{II}, $ECOP_{TOT}$, EPC_{TOT}, and ExD_{TOT} and lower s_{gen_TOT} compared to R290, R152a, and R134a. This suggests that R717 is more efficient in converting waste heat into refrigeration, indicating that ammonia might be a slightly more efficient refrigerant in this specific application, despite its disadvantages for human health.

Temperature (T), pressure (P), specific enthalpy (h), specific entropy (s), mass flow rate (m), specific volume (v), specific exergy (ex), and exergy density (ρ_{Ex}) values of system points for the R717 are presented in Table 3 as thermophysical properties. Our priorities are to maximize practical work production, minimize energy losses, and reduce environmental impacts. In this case, the advantages of R717 refrigerant, which has the highest total *ECOP* and *EPC* values, are apparent.

To evaluate the system's overall performance, it would be helpful to calculate the performance outputs that would

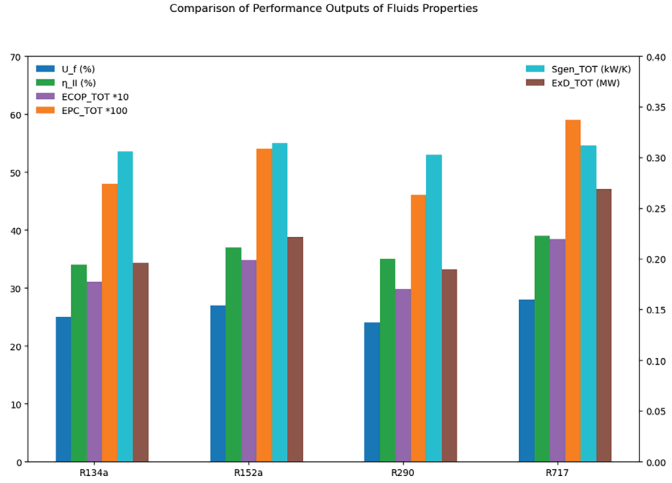


Figure 2. Comparison of performance outputs of different fluids.

η_{II}: Second law efficiency, s_{gen_TOT}: Total entropy generation, $ECOP_{TOT}$: Ecological coefficient of performance, EPC_{TOT}: Exergetic performance criteria, ExD_{TOT}: The exergy destruction, U_f: Utility factor

provide a comprehensive understanding of the system's losses and efficiencies. Table 4 represents performance outputs such as *ExD*, *EPC*, *y*, and η_{II} for the heat-powered MRS components (steam turbine, compressor, condenser, evaporator, expansion valve, pump, and boiler). The table shows that the evaporator has the highest ExD_{TOT} rate and the highest y value, with an almost 41% ratio, and the lowest *ExD* and *y* values belong to the pump unit. It can also be obtained from the table that the heat-related components (condenser, evaporator, and boiler) generate more ExD_{TOT}. Regarding the EPC value, the highest values are for pump and turbine units; the lowest are for heat-related units. By implementing design modifications and operational adjustments to the evaporator, condenser, and boiler units, the system's ExD_{TOT} can be reduced, leading to a notable increase in overall efficiency.

Figure 3 shows the effect of the $T_{Turbine}$ on the system components' *EPC*. As the $T_{Turbine}$ increases, the overall *EPC* generally decreases. Nevertheless, the individual *EPC* contributions of different components demonstrate different

Table 3. Thermophysical properties of system points.

No	*T* (K)	*P* (kPa)	*h* (kJ/kg)	*s* (kJ/kg K)	*m* (kg/s)	*v* (m³/kg)	*ex* (kJ/kg)	ρ_{ex} (MJ/m³)
1	318.15	1,781.67	560.67	2.20	1.654	0.002	324.84	185.62
2	318.15	1,781.67	560.67	2.20	0.348	0.002	324.84	185.62
3	258.15	236.11	560.67	2.33	0.348	0.11	288.72	2.600
4	258.15	236.11	1,589.68	6.31	0.348	0.51	129.92	0.260
5	429.71	1,781.67	1,896.97	6.44	0.348	0.11	452.88	4.050
6	318.15	1,781.67	560.67	2.20	1.306	0.002	324.84	185.62
7	319.47	5,116.42	566.81	2.21	1.306	0.002	330.73	189.65
8	363.15	5,116.42	1,604.99	5.11	1.306	0.02	504.59	21.95
9	318.15	1,781.67	1,483.68	5.16	1.306	0.06	384.43	6.050

T: Temperature, *P*: Pressure, *h*: Specific enthalpy, *s*: Specific entropy, *m*: Mass flow rate, *v*: Specific volume, *ex*: Specific exergy, ρ_{Ex}: Exergy density

Table 4. Performance outputs of the system using R717 for given conditions.

Component	*ExD* (kW)	*EPC*	*y*
Turbine	22.26	28.61	0.083
Compressor	13.41	11.74	0.05
Condenser	53.63	13.30	0.2
Evaporator	110.42	0.41	0.410
Expansion valve	12.56	7.99	0.047
Pump	1.27	340.22	0.005
Boiler	55.18	11.94	0.205

ExD: The exergy destruction, EPC: Exergetic performance criteria, *y*: Exergy destruction ratio

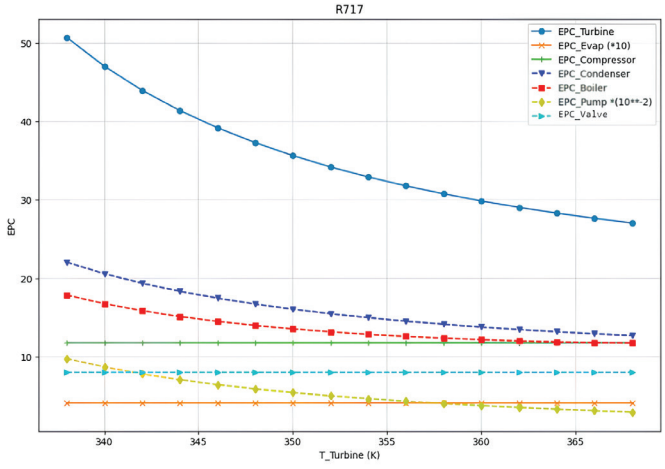


Figure 3. The turbine temperature effects on the EPC values.

EPC: Exergetic performance criteria

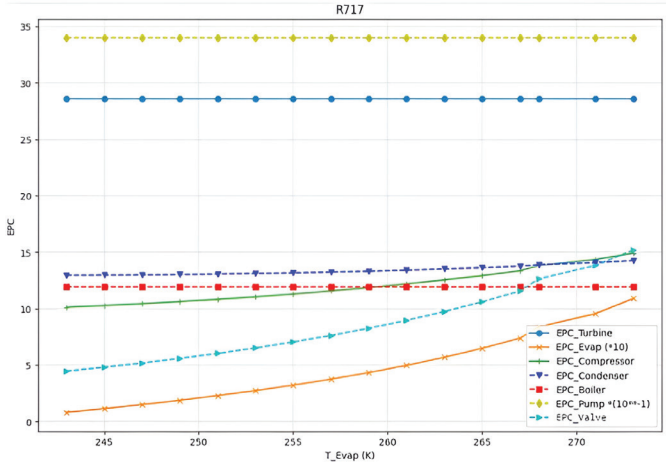


Figure 4. The evaporator temperature effects on the EPC values.

EPC: Exergetic performance criteria

trends. Significant decreases in $EPC_{Turbine}$, EPC_{Boiler}, and $EPC_{Condenser}$ between 340 and 355 K temperature and slight decreases in EPC_{Pump} are also observed. EPC_{Evap}, $EPC_{Compressor}$, and EPC_{Valve} remain relatively constant, as the evaporator's temperature does not directly affect the compressor's and valve's performance.

Figure 4 shows the effect of T_{Evap} on the *EPC* of the system components. As the T_{Evap} increases, the overall *EPC* generally increases. However, the individual *EPC* contributions of different components show different trends. $EPC_{Turbine}$, EPC_{Boiler}, and EPC_{Pump} remain relatively constant, as the turbine's, boiler's, and pump's performance are not directly

affected by the T_{Evap}. EPC_{Evap} and $EPC_{Condenser}$ increase slightly, $EPC_{Compressor}$ and EPC_{Valve} increases significantly with T_{Evap}.

Figure 5 shows the relationship between the U_f and the total EPC_{TOT} or EPC_{TOT} where the different lines represent various combinations of evaporator and $T_{Turbine}$. As the T_{Evap} increases, the EPC_{TOT} generally decrease for a given U_f, and the U_f increases for a given constant $T_{Turbine}$. However, there is a trade-off between T_{Evap} and cooling capacity. Higher T_{Evap} can reduce the cooling capacity of the system. Increasing the $T_{Turbine}$ generally increases EPC_{TOT} and U_f for constant T_{Evap}. Since improving EPC_{TOT} is the priority, the scenario in which It reaches its maximum improvement should be considered. Therefore, when the T_{Evap} was set to 243.15 K and the $T_{Turbine}$ to 368.15 K, an improvement of nearly 100% in EPC_{TOT} and almost 115% in U_f according to the values in $T_{Turbine}$ is 338.15 K.

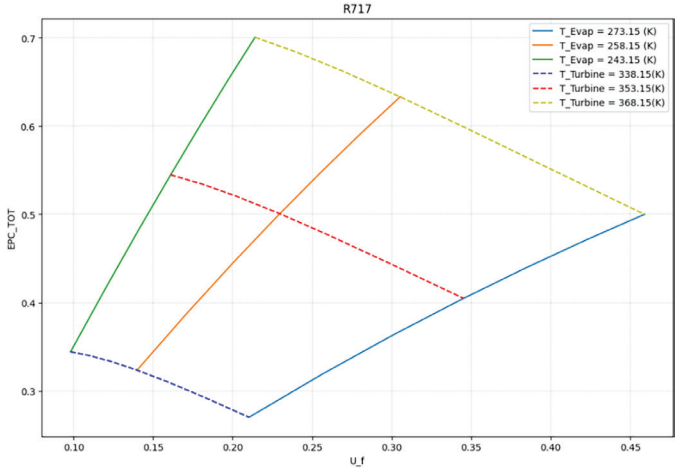


Figure 5. The turbine and evaporator temperatures effects on the U_f and EPC_{TOT}.

U_f: Utility factor, EPC_{TOT}: Exergetic performance criteria

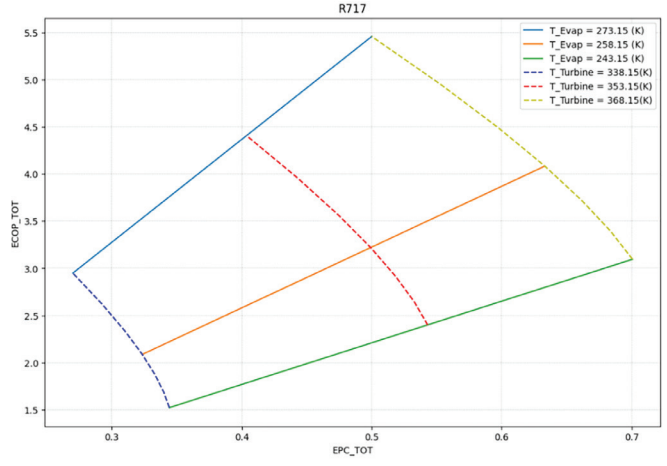


Figure 6. The turbine and evaporator temperatures effects on the EPC_{TOT} and $ECOP_{TOT}$.

EPC_{TOT}: Exergetic performance criteria, $ECOP_{TOT}$: Ecological coefficient of performance

Figure 6 depicts the effects of the evaporator and $T_{Turbine}$ on the relationship between $ECOP_{TOT}$ or $ECOP_{TOT}$ and EPC_{TOT}. As the T_{Evap} increases, the $ECOP_{TOT}$ generally increases for a given EPC_{TOT} or at a constant $T_{Turbine}$. However, increasing in T_{Evap} at constant $T_{Turbine}$ decreases the EPC_{TOT}. T_{Evap} and cooling capacity are inversely correlated, such that an increase in one leads to a decrease in the other. Increasing the $T_{Turbine}$ generally leads to a increase in $ECOP_{TOT}$ for a constant T_{Evap}. The ideal scenario is when the T_{Evap} is 258.15 K, and the $T_{Turbine}$ is 368.15 K to maintain optimal improvements in both $ECOP_{TOT}$ and EPC_{TOT}.

Figure 7 describes the relationship between EPC_{TOT} and η_{II} of the system using R717. As the T_{Evap} increases, η_{II} generally increases while EPC_{TOT} decreases for constant $T_{Turbine}$. Increasing the $T_{Turbine}$ generally increases both EPC_{TOT} and η_{II} for a given T_{Evap}. Since maximizing EPC_{TOT} is the primary objective, the scenario yielding its highest improvement should be considered. Accordingly, when the T_{Evap} was adjusted to 243.15 K and the $T_{Turbine}$ was 368.15 K, an enhancement of almost 170% in η_{II} was calculated by comparing it to the lowest scenario.

Figure 8 depicts the relationship between EPC_{TOT} and ExD_{TOT}. The different lines represent various combinations of evaporator and $T_{Turbine}$. As the T_{Evap} increases, the ExD_{TOT} generally increases for a given EPC_{TOT}, and EPC_{TOT} decreases with higher T_{Evap} at a constant $T_{Turbine}$ value. Increasing the $T_{Turbine}$ generally increases the ExD_{TOT} and EPC_{TOT}. By carefully selecting these temperatures, optimizing the system's performance in terms of both ExD_{TOT} and EPC_{TOT} is possible. While improving EPC_{TOT}, to keep ExD_{TOT} at its lowest level, two scenarios emerge: The most optimal

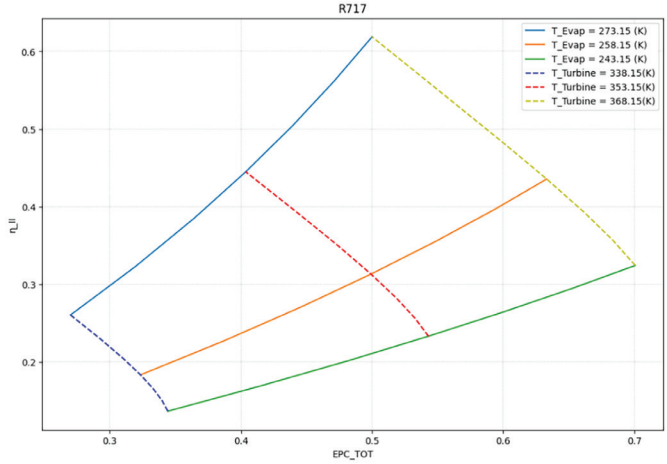


Figure 7. The turbine and evaporator temperatures effects on the η_{II} and EPC_{TOT}.

η_{II}: Second law efficiency, EPC_{TOT}: Exergetic performance criteria

balance between both values occurs when the T_{Evap} is 243.15 K and the $T_{Turbine}$ is 338.15 K. However, if the increase in ExD_{TOT} can be overlooked, the ideal temperature range for maximizing EPC_{TOT} is when the T_{Evap} is 243.15 K and the $T_{Turbine}$ is 368.15 K.

Figure 9 shows the relationship between EPC_{TOT} and s_{gen_TOT} for the system according to the different T_{Evap} (straight lines) and $T_{Turbine}$ (dotted lines). As the T_{Evap} increases, the s_{gen_TOT} generally increases for a given EPC_{TOT}. However, EPC_{TOT} also decreases with higher T_{Evap}. Higher T_{Evap} can lead to higher irreversibilities in the system, such as heat transfer across finite temperature differences and pressure drops in the components. Increasing the $T_{Turbine}$ generally leads to an increase in s_{gen_TOT} for a given EPC_{TOT}. Besides, EPC_{TOT} also

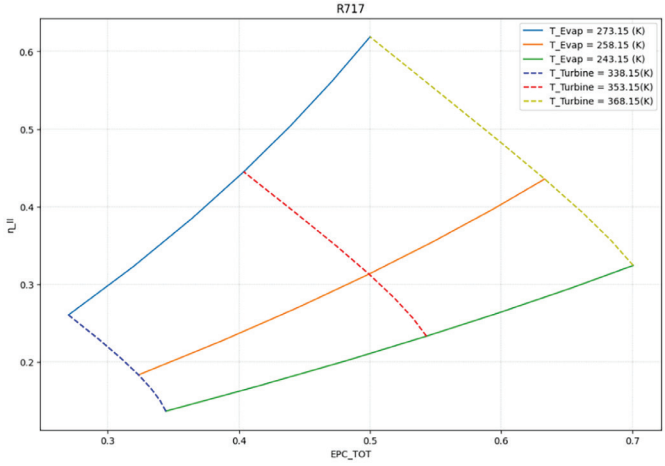


Figure 8. The turbine and evaporator temperatures effects on the ExD_{TOT} and EPC_{TOT}.

EPC_{TOT}: Exergetic performance criteria, ExD_{TOT}: The exergy destruction

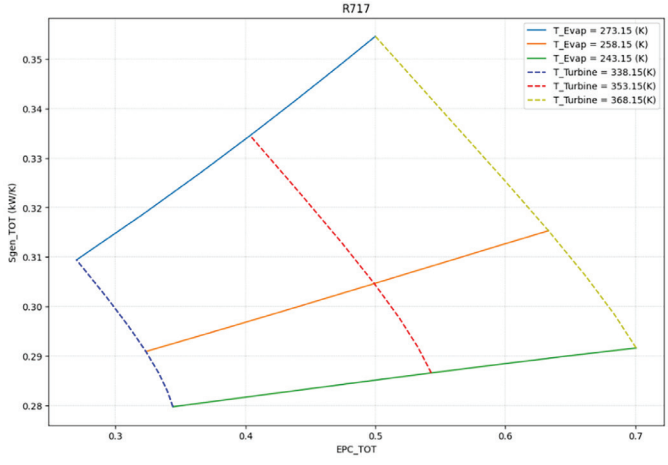


Figure 9. The turbine and evaporator temperatures effects on the s_{gen_TOT} and EPC_{TOT}.

s_{gen_TOT}: Total entropy generation, EPC_{TOT}: Exergetic performance criteria

increases with higher $T_{Turbine}$. The optimal combination of evaporator and $T_{Turbine}$ depends on the specific requirements of the heat-powered refrigeration system, which must balance between minimizing s_{gen_TOT} and maximizing EPC_{TOT}. For example, lower $T_{Turbine}$ and T_{Evap} might be suitable if the priority is to minimize entropy generation. If the priority is to maximize EPC_{TOT}, a lower v and a higher $T_{Turbine}$ might be better. It has been observed that the ideal scenario between EPC_{TOT} and s_{gen_TOT} occurs when the T_{Evap} is 243.15 K, and the $T_{Turbine}$ is 368.15 K.

4. Conclusion

This study investigated the feasibility of converting waste heat from ship exhaust gas into helpful energy through an ORC and subsequently utilizing this converted energy in a VCR cycle. The effects of the varying evaporator and condenser temperatures and different working fluids on the U_f, η_{II}, and s_{gen_TOT} production were analyzed. The results indicated that ammonia (R717) is the most suitable fluid for this system. Future research endeavors will focus on conducting detailed comparative performance analyses and exploring exergy-based environmental and economic assessments. Analyses have shown that the high *ECOP* and EPC values of R717 (ammonia) indicate their significant potential to enhance system efficiency. These results suggest that R717 could play an effective role in energy conversion processes, particularly optimizing energy efficiency. Furthermore, the high efficiency of R717 could lead to lower emissions and more sustainable energy solutions from an environmental perspective, while economically, it could reduce operating costs by lowering energy consumption. Future studies will further explore the broader application areas of R717 and its impact on environmental and economic assessments.

The optimal combination of e T_{Evap} and $T_{Turbine}$ depends on the specific requirements of the refrigeration system. For example, if the priority is to maximize cooling capacity, a lower T_{Evap} and a higher $T_{Turbine}$ might be suitable. If the priority is to minimize energy consumption, a higher T_{Evap} and a lower $T_{Turbine}$ might be better. Figures 5-9 show that the EPC_{TOT} of the heat-powered system using R717 is influenced by both the evaporator and $T_{Turbine}$. To optimize the total EPC, it is advantageous to operate at a lower T_{Evap} and a higher $T_{Turbine}$. The observations indicate that the optimal thermodynamic conditions for the EPC_{TOT}, occur at an T_{Evap} of 243.15 K and a $T_{Turbine}$ of 368.15 K which have almost 100% increment according to the lowest EPC_{TOT} value. By carefully selecting these temperatures, optimizing the system's performance for a given application is possible.

NOMENCLATURE

Symbol	Name
Cp	The specific heat capacity at constant pressure
ECOP	Ecological coefficient of performance
EPC	Exergetic performance criteria
η_{II}	Second law efficiency
ex	Specific exergy
ExD	Exergy destruction
GWP	Global warming potential,
h	Specific enthalpy
ORC	Organic Rankine cycle
m	Mass flow rate
MRS	Marine refrigeration system
P	Pressure
RL	Refrigeration loop
RCL	Refrigerant concentration limit
ρ_{ex}	Exergy density
s	Specific entropy
s_{gen_TOT}	Total entropy generation
T	Temperature
Q	The heat transfer ratio
U_f	Utility factor
W	Net work
v	Specific volume
VCR	Vapor compression refrigeration
y	Exergy destruction ratio
	Subscripts
0	Dead state conditions
avr	Average
c	Compressor
Con	Condenser
env	Environment
Evap	Evaporator
H	High temperature, Heat input
in	Inlet
L	Low temperature, Heat output
p	Pump
out	Outlet
sys	System
TOT	Total
Gen	Generated

Acknowledgement

The short version of this study was presented at the Fourth International Naval Architecture and Maritime Symposium (INTNAM-2023, YTÜ, İstanbul, 11-13.10.2023), the present paper is the improved version in terms of analysis and content. We would like to thank those who contributed to the symposium organisers and the journal publication process.

Footnotes

Authorship Contributions

Concept: O. Yılmaztürk, Design: O. Yılmaztürk, Data Collection or Processing: O. Yılmaztürk, and A. S. Karakurt, Analysis or Interpretation: A. S. Karakurt, Literature Review: O. Yılmaztürk, and A. S. Karakurt, Writing: O. Yılmaztürk, and A. S. Karakurt.

Conflict of Interest: No conflict of interest was declared by the authors.

Financial Disclosure: The authors declared that this study received no financial support.

References

[1] L. A. Díaz-Secades, R. González, N. Rivera, E. Montañés, and J. R. Quevedo, "Waste heat recovery system for marine engines optimized through a preference learning rank function embedded into a Bayesian optimizer," *Ocean Engineering*, vol. 281, 114747, Aug 2023.

[2] A. S. Karakurt, B. Başaran, and E. Z. Çubukçu, "Performance analyses of marine thermal oil system," *Gemi ve Deniz Teknolojisi,* no. 222, pp. 196-208, Jan 2023.

[3] B. Khan, and M.-H. Kim, "Energy and exergy analyses of a novel combined heat and power system operated by a recuperative organic rankine cycle integrated with a water heating system," *Energies*, vol. 15, no. 18, 6658, Jan 2022.

[4] T. Koroglu, I. Cavus, and M. U. Bayer, "Marine engine efficiency improvement with supercritical-CO2 Rankine waste heat recovery," *International Journal of Exergy,* vol. 40, no. 3, pp. 347-364, Jan 2023.

[5] V. Başhan, and A. Parlak, "Economic analysis of a ship refrigeration system in case of variable sea water temperature conditions," *Journal of ETA Maritime Science*, vol. 3, no. 2, pp. 67-74, 2015.

[6] R. Tozer, and R. W. James, "Heat powered refrigeration cycles," *Applied Thermal Engineering,* vol. 18, no. 9, pp. 731-743, Sep 1998.

[7] S. Khatoon, N. M. A. Almefreji, and M.-H. Kim, "Thermodynamic study of a combined power and refrigeration system for low-grade heat energy source," *Energies*, vol. 14, no. 2, pp. 410, Jan 2021.

[8] A. Elbir, F. A. Kodaloglu, I. Ucgul, and M. E. Sahin, "Thermodynamic analysis of refrigerants used in ORC-VCC combined power systems for low temperature heat sources," *Thermal Science,* vol. 26, no. 4 Part A, pp. 2855-2863, 2022.

[9] R. Zhar, A. Allouhi, A. Jamil, and K. Lahrech, "Performance analysis of combined power and refrigeration: ORC-VCC system," in *WITS 2020*, S. Bennani, Y. Lakhrissi, G. Khaissidi, A. Mansouri, and Y. Khamlichi, Eds., in Lecture Notes in Electrical Engineering. Singapore: Springer, 2022, p. 595-605.

[10] Y. Liang, Z. Yu, and W. Li, "A waste heat-driven cooling system based on combined organic rankine and vapour compression refrigeration cycles," *Applied Sciences*, vol. 9, no. 20, 4242, Jan 2019.

[11] X. Xia, Z. Liu, Z. Wang, T. Sun, and H. Zhang, "Multi-layer performance optimization based on operation parameter-working fluid-heat source for the ORC-VCR system," *Energy*, vol. 272, 127103, Jun 2023.

[12] O. Bounefour, A. Ouadha, and Y. Addad, "An exergy analysis of various layouts of ORC-VCC systems for usage in waste heat recovery onboard ships," *Marine Systems & Ocean Technology,* vol. 15, no. 1, pp. 26-44, Mar 2020.

[13] C. Aktemur, and G. Hacipasaoglu, "Assessment of an integrated organic rankine cycle (ORC)-vapor compression refrigeration (VCR) system using the energy, conventional exergy, and advanced exergy analysis," *Heat Transfer Research,* vol. 52, no. 15, 2021.

[14] M.-H. Kim, "Energy and exergy analysis of solar organic rankine cycle coupled with vapor compression refrigeration cycle," *Energies*, vol. 15, no. 15, Jan 2022.

[15] Y. Liang, A. Mckeown, Z. Yu, and S. F. K. Alshammari, "Experimental study on a heat driven refrigeration system based on combined organic Rankine and vapour compression cycles," *Energy Conversion and Management,* vol. 234, 113953, Apr 2021.

[16] Y. Ust, "Performance analysis and optimization of irreversible air refrigeration cycles based on ecological coefficient of performance criterion," *Applied Thermal Engineering,* vol. 29, no. 1, pp. 47-55, Jan 2009.

[17] Y. Ust, A. S. Karakurt, and U. Gunes, "Performance analysis of multipurpose refrigeration system (MRS) on fishing vessel," *Polish Maritime Research,* vol. 23, no. 2, pp. 48-56, 2016.

[18] L. Chen, Y. Ge, S. Shi, H. Feng, and P. Liu, "Exergetic efficiency and exergy-based ecological function performance optimizations for two irreversible simple Brayton refrigeration cycle models," *Results in Engineering*, vol. 22, 101967, Jun 2024.

[19] Md. M. Arefin, D. Mondal, and Md. A. Islam, "Optimizing cascade refrigeration systems with low GWP refrigerants for low-temperature applications: A thermodynamic analysis," *Energy Conversion and Management: X,* vol. 24, 100722, Oct 2024.

[20] Y. Ust, and A. S. Karakurt, "Analysis of a cascade refrigeration system (CRS) by using different refrigerant couples based on the exergetic performance coefficient (EPC) criterion," *Arabian Journal for Science and Engineering,* vol. 39, no. 11, pp. 8147-8156, Nov 2014.

[21] O. Yilmazturk, and A. S. Karakurt, "*Analyses of an ideal combined heat-powered marine refrigeration system,*" presented at the 4th International Naval Architecture and Maritime Symposium (Int-Nam 2023), İstanbul, Oct 2023. Accessed: Sep 13, 2024. [Online]. Available: https://avesis.yildiz.edu.tr/yayin/4e11e10f-2bff-4fea-b347-43e870e4a316/analyses-of-an-ideal-combined-heat-powered-marine-refrigeration-system

[22] A. S. Karakurt, and B. Sahin, "A new method for the size and performance analyses and optimization of thermal systems: The exergy density," *Sigma Journal of Engineering and Natural Sciences,* vol. 37, no. 2, pp. 573-583, Jul 2019.

[23] A. Bejan, "Entropy generation minimization: The new thermodynamics of finite-size devices and finite-time processes," *Journal of Applied Physics,* vol. 79, no. 3, pp. 1191-1218, Feb 1996.

[24] Y. Ust, B. Sahin, and A. Kodal, "Ecological coefficient of performance (ECOP) optimization for generalized irreversible Carnot heat engines," *Journal of the Energy Institute,* vol. 78, no. 3, pp. 145-151, Aug 2005.

[25] Y. Ust, B. Sahin, and T. Yilmaz, "Optimization of a regenerative gas-turbine cogeneration system based on a new exergetic performance criterion: Exergetic performance coefficient," *Proceedings of the Institution of Mechanical Engineers Part A-Journal of Power and Energy,* vol. 221, no. 4, pp. 447-456, Jun 2007.

[26] ASHRAE, *Designation and Safety Classification of Refrigerants*, Standart 34, Georgia, US., 2019. [Online]. Available: https://www.ashrae.org/technical-resources/bookstore/standard-34-designation-and-safety-classification-of-refrigerants

[27] I. H. Bell, J. Wronski, S. Quoilin, and V. Lemort, "Pure and pseudo-pure fluid thermophysical property evaluation and the open-source thermophysical property library CoolProp," *Industrial & Engineering Chemistry Research,* vol. 53, no. 6, pp. 2498-2508, Feb 2014.